SAND2008-1194C

# MODELING OF HEAVY ION INDUCED CHARGE LOSS MECHANISMS IN NANOCRYSTAL MEMORY CELL

**A. Cester, N. Wrachien, DEI, Università di Padova, Padova, Italy**

**J. Schwank, G. Vizkelethy, Sandia National Laboratories, Albuquerque, NM**

**R. Portoghese, C. Gerardi, ST Microelectronics, Catania, Italy**

**35-word abstract**

**We present the first charge loss model on nonvolatile nanocrystal memories. It predicts the threshold voltage dependence on the ion hit number and position. It also provides an estimation of the ion hit track size.**

**Corresponding Author:**
Andrea Cester, Dipartimento di Ingegneria dell'Informazione – Università di Padova,
via Gradenigo 6/B, 35131 Padova, Italy,
phone: +39 049 827 7787, fax: +39 049 827 7699,
email: andrea.cester@dei.unipd.it

**Contributing Authors:**
Nicola Wrachien, Dipartimento di Ingegneria dell'Informazione – Università di Padova, Italy.
email: wrachien@dei.unipd.it

Alberto Gasperin, Dipartimento di Ingegneria dell'Informazione – Università di Padova, Italy
email: alberto.gasperin@dei.unipd.it

James R. Schwank, Sandia National Laboratories, Albuquerque, NM
email: schwanjr@sandia.gov

Gyorgy Vizkelethy, Sandia National Laboratories, Albuquerque, NM
email: gvizkel@sandia.gov

Rosario Portoghese, STMicroelectronics, Catania, Italy,
email : rosario.portoghese@st.com

Cosimo Gerardi, STMicroelectronics, Catania, Italy,
email : cosimo.gerardi@st.com

**Section Preference:** "Single Event Effect: Mechanisms and Modelling" OR "Device and IC's"

**Presentation Preference:** Oral

## I. INTRODUCTION

Several reliability constraints are hampering the scaling of the floating gate memories (FGM) along the ITRS roadmap. The data retention requirements, the presence of fast and erratic bits, and the drain-induced turn-on are limiting the tunnel oxide shrinking to 7-8nm [1]. Moreover, FGMs show a limited tolerance against ionizing radiation in terms of total ionizing dose and single event effects [2-4]. Many alternatives are currently being considered, exploring both new materials (e.g., ferroelectrics and chalcogenides, etc.) and new cell structures [5]. Among them, nanocrystal memory (NCM) represents the most natural and cost-effective solution, because they can be cheaply fabricated using a standard CMOS process flow, with only few added masks. In fact, in NCMs the monolithic floating gate (FG) is replaced with a layer of discrete nanocrystals (NCs). This permits to scale the dielectric thickness down to 4-5nm [6] and to employ low programming voltages and short programming time [7].

It has been recently shown that NCM increases the tolerance against both SILC and RILC, because a single weak spot in the tunnel oxide can discharge only the few neighboring nanocrystals, leading to a limited threshold voltage variation. In a previous work [8] we analyzed the effect of one/few ion hits on addressable arrays using a broad beam of heavy ions. Unfortunately, with such ion beam the whole chip is irradiated, including all the peripheral circuitry (control circuitry, decoders, etc). Consequently, the ion fluence must be kept low enough to avoid any appreciable radiation damage in the peripheral circuitry. Despite these limits, we demonstrated that a single ion hit does not produce any appreciable change in the threshold voltage as long as the cell size is larger than the ion track size.

A fine estimation of the threshold voltage variation induced by a given number of ion hits is a very complex task, which requires to know the NC charge state and distribution over the device area, the ion track size, and the effects of a single discharged NC on the oxide electric field. At present, there are no models that allow the prediction of the threshold voltage variation on NCMs after a heavy ion irradiation.

## II. AIM OF THE WORK

*In this work we aim to model the prompt charge loss induced by heavy ion irradiation. Our purpose is to calculate the threshold voltage variation of the hit cells depending on the number of ion hits, the ion track size, the initial nanocrystal charge, and the amount of charge loss. We used the microbeam facility at the Sandia National Laboratories, which permits the accurate estimation of the irradiated area, and it permits to rise the fluence levels, enabling the study of the impact of multiple ion hits.*

## III. EXPERIMENTALS AND DEVICES

We analyzed 16Mbit NCM arrays organized in 32 blocks of 512kbits. Each block is divided in 8 sectors of 64kbits. The cells aspect ratio is W/L = 200nm/300nm, the tunnel oxide thickness is 5nm, the control dielectric consists of an Oxide-Nitride-Oxide (ONO) stack with an equivalent oxide thickness (EOT) of 12nm. The average nanocrystal diameter and density have been estimated through TEM measurements and they are 6nm and $5 \cdot 10^{11}$ $cm^{-2}$, respectively (see Fig. 1 for further details). The cell erasure and program were performed by Fowler-Nordheim (FN) injection and CHannel Initiated Secondary Electron injection (CHISEL), respectively [7].

The irradiation experiments were performed at the Sandia National Laboratories (Albuquerque, NM), using a focused Cu ion beam (surface LET = 33.5 $MeV \cdot cm^2 \cdot mg^{-1}$, Energy = 50 MeV). The devices were irradiated unbiased. This is a good approximation of the real operating condition because each memory cell is left in high impedance state for the majority of its lifetime, and it is accessed only occasionally. In each array, one half of cells were programmed at "1" and one half at "0" with a checkerboard pattern.

## IV. RESULTS

In Fig. 2 we show the threshold voltage ($V_{TH}$) distribution before and after irradiation with $1.67 \cdot 10^9$ Cu ions/$cm^2$. The sector area is $5.38 \cdot 10^{-4}$ $cm^{-2}$, but the ion beam was focused on a smaller area ($3.15 \cdot 10^{-4}$ $cm^{-2}$). We chose the ion fluence so that, namely, the 100% of cells received one hit within the irradiated area. The threshold voltage has been defined as the gate voltage required by the cell for driving a drain current $I_{DS}$= 20μA (at $V_{DS}$ = 0.8V). The deviation from the typical behavior mainly derives from the process parameter dispersion, the local variation of the nanocrystal density, and the position of the cell within the array, which differently impacts on the cell parasitics. The heavy ion exposure has negligible effects on the erased cells, because the stored charge is almost neutral, as already discussed in [8]. On the contrary, the programmed cell distribution feature a large tail after irradiation, as can be seen in the cumulative probability distribution in

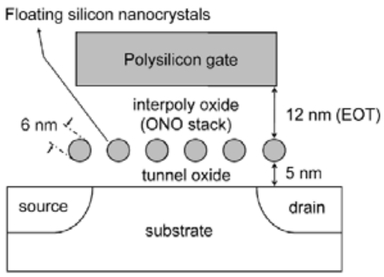


Fig. 1. Cross section of a NCM cell used in this work.

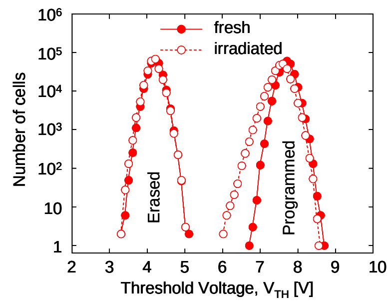


Fig. 2. Threshold voltage distribution of a fresh and irradiated NCM array.

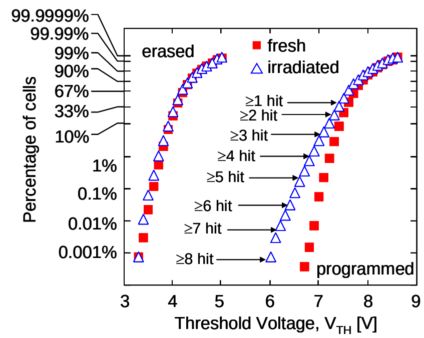


Fig. 3. Cumulative probability distribution of the same irradiated cell array of Fig. 2.

Fig. 3. The 8 arrows in Fig. 3 represent the cumulative probability that at least 1,2,3, … ions hit a single cell. This calculation has been done using the model proposed in [8] and taking into account that only a fraction of the sector was effectively irradiated (58.6%). The  shift between the fresh and irradiated device curves in Fig. 3 is 18mV at the probability of 1 hit, 0.3V at 3 hits, and increases up to 0.72V at 8 hits. Hence, a single ion hit cannot produce a substantial $V_{TH}$ shift, and even after 8 hits the programmed cell distribution is still not-overlapping with the erased cell distribution.

As discussed in [8] the origin of such tail is the prompt charge loss due to several mechanism: the photoemission and the recombination with the charge generated in the oxide within the ion track; and (at less degree) the transient conductive path.

## V. MODELING AND SIMULATIONS

The purpose of our model is to simulate the variation of the array $V_{TH}$ distribution after heavy ion irradiation, given the nominal ion fluence. This task is relatively simple in FGM, because the $V_{TH}$ shift induced by the ion strikes is independent on the hit position along the channel (being metallic the floating gate behavior). Instead, in a NCM cell each ion hit discharges only the neighboring NCs, and the stored charge does not redistribute. Consequently, the $V_{TH}$ locally changes only around the hit positions. To produce an appreciable cell $V_{TH}$ reduction, the ion hits must be contiguous each other along the channel, and they must form a percolation path from the source to the drain diffusion (see Fig. 4).

In the following we summarize our model in two steps: firstly we consider the NCM cell electrostatics, which permits us to simulate the $I_{DS}$-$V_{GS}$ characteristics once the position and the electric charge of each NC are known. Our model works with arbitrary NC charge and spatial distributions. Secondly, a Monte Carlo based simulation is used to simulate the ion hit effects.

### *A. Channel electrostatics and conduction modeling*

Our electrostatic model is based on the following assumptions (see Fig. 5a):

A1) The gate and the channel in linear region are approximated as an infinite metallic sheet. This is a good approximation for all NCs in the center of the channel, but it is less accurate for the NCs on the channel edges. However, we verified that the edge-NCs have a minor impact on the whole channel conductance.

A2) Each charged NC is approximated as a point charge.

A3) The normal component of the electric field ($E_{ox}$) is much larger than the longitudinal component ($\boldsymbol{E_L}$).

Following assumption A1, the polysilicon gate and the strongly inverted channel act as a metal plate. Therefore, we studied a linear system of charges and conductors and we adopted the method of the superposition of the effects to evaluate the normal electric field ($E_{ox}$) all over the channel area. Using the image charge method, we evaluated the electric field at the substrate-oxide interface induced by a single NC charged with an elementary negative charge. This is calculated as a sum of infinite terms of image charges, corresponding to infinite reflections of the nanocrystal charge at the two electrodes (see Fig.5a for notations):

$$E_{ox}(r)=\frac{-q}{4\pi\varepsilon_{ox}}\left[\frac{1}{\left(r^2+t_1^2\right)}+\sum_{n=0}^{\infty}\left(\frac{-1}{r^2+\left(t_1+2n\left(t_1+t_2\right)\right)^2}+\frac{-1}{r^2+\left(t_1+2t_2+2n\left(t_1+t_2\right)\right)^2}+\frac{1}{r^2+\left(t_1+2t_2+2n\left(t_1+t_2\right)\right)^2}+\frac{1}{r^2+\left(3t_1+2t_2+2n\left(t_1+t_2\right)\right)^2}\right)\right]$$

We limited the number of terms of the sum accordingly to the desired approximation (we chose $10^{-4}$%). Despite its simplicity, the results of our electrostatic model, combined with the heavy ion modeling (see next subsection), are in excellent agreement with the experimental data. In addition, thanks to our assumptions, the model needs to calculate the NC-induced electric field only once, shortening the simulation time.

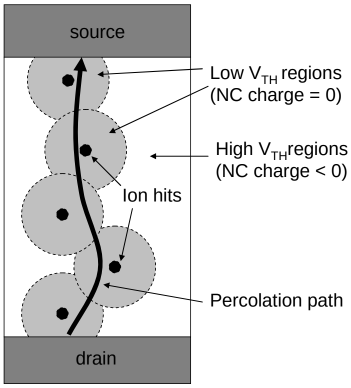

Fig. 4. Percolation path formation along the MOSFET channel following multiple hits.

Once the normal electric field $E_{ox}$ is calculated at the position *(x,y)* along the channel, we evaluated the local carrier density per unit of area $n_S(x,y)$ and the local channel conductance $\sigma_S(x,y)$ per unit of area:

$$\sigma_S(x,y) = \mu \cdot q \cdot n_S(x,y) = \mu \cdot E_{ox}(x,y) \cdot \varepsilon_o$$

$\mu$ is the electron mobility; $\varepsilon_{ox}$ is the oxide dielectric permittivity; and $q$ is the elementary charge.

From assumption A3, the longitudinal component of the channel electric field $\mathbf{E_L}$ can be calculated by the ohm law, in the 2D system, neglecting the effect of $\mathbf{E_L}$ on the free carrier density:

$$\mathbf{J}(x,y) = \sigma(x,y)\mathbf{E_L}(x,y)$$

By imposing the charge conservation:

$$div(\mathbf{J}) = div(\sigma \mathbf{E_L}) = \mathbf{E_L} \bullet grad(\sigma) + \sigma div(\mathbf{E_L}) = 0$$

The solution of this system has been numerically calculated over a mesh grid with 1-nm width (the detail will be shown in the final paper, due to lack of space). The device parameters ($\mu$, $C_{ox}$, etc) have been calibrated to fit the $I_{DS}$-$V_{GS}$ characteristics of a single NCM cell. Fig. 6 shows the good fit between our model and the experimental results on a neutral and a programmed cell.

This model can evaluate the $I_{DS}$-$V_{GS}$ characteristics for arbitrary NC arrangement and NC charge distribution. Nonetheless, for simplicity and brevity, in the following we will discuss the case of regularly spaced and uniformly charged NC (see Fig. 5b). This is an approximation of the real NC distribution, but it has a modest impact on our results. In fact, the NC non uniformity induces a potential perturbation much smaller than the variation induced by NC charge loss due to the ion hit. We postpone the discussion of the effect of NC distribution and charges to the final paper.

### *B. Radiation Damage Modeling*

Once the electrostatic model of the NCM cell has been assessed, we consider the effects of the ion hits. At this purpose we made some additional assumptions (see Fig. 5b):

B1) For simplicity, each ion hit discharges all the NCs within a circular area with diameter S, while all the charges stored outside this area are unchanged.

B2) The probability that a cell experiences M ion hits is calculated using the model proposed in [8] and taking into account the effective irradiation spot size.

B3) The NCs are uniformly charged, which is good approximation in case of FN injection. Simulations are running (and they will be shown in the final paper) to take into account the non uniformity of the NC stored charge due to CHISEL program technique.

The way the ion hits modify the cell $I_{DS}$-$V_{GS}$ is very different and it strongly depends on the ion hit positions. Let us consider, for instance, Fig. 7. Here we show two examples of quadruple hit patterns representing two opposite cases (see Figs. 7a and 7c). We assumed the spot size of each ion hit S=100nm. In Fig. 7e we show the $I_{DS}$-$V_{GS}$ of a neutral device (dashed), a programmed device (solid) and two cell hit by 4 ions (solid line marked with #1 and #2). In the case #1, a percolation path exists between source and drain (Fig. 7b) and the cell turns on earlier than the fresh cell. Instead, in case #2 the ion hit positions are very close each other and they are not able to generate any percolation path (Fig. 7d). The cell $V_{TH}$ reduces, but it is less affected than in case #1. This phenomenon does not occur on conventional FGMs, because the $V_{TH}$ variation mostly depends on the number of hits and not on their positions.

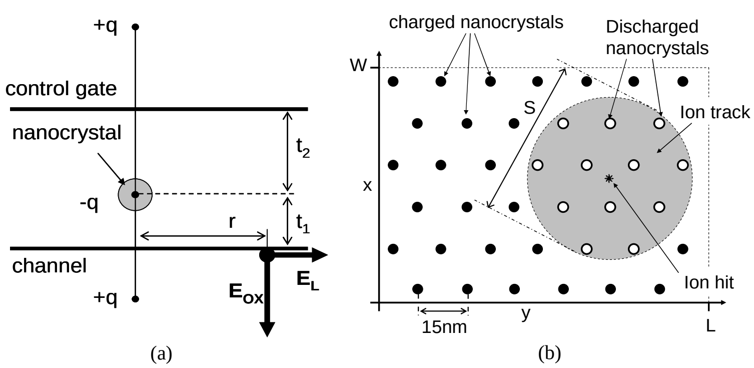

Fig. 5. a) Nanocrystal electrostatic model and notations. Only the image charge of the first reflection are shown, for simplicity. b) Uniform nanocrystal distribution with centered body hexagonal pattern .

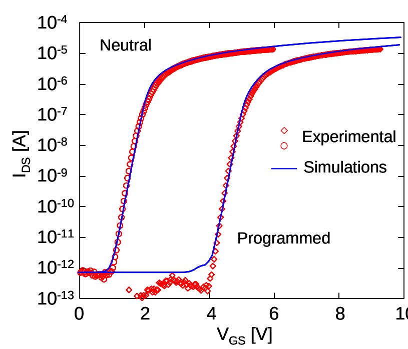

Fig. 6. Comparison between model and the experimental measurements of a programmed and a neutral cell.

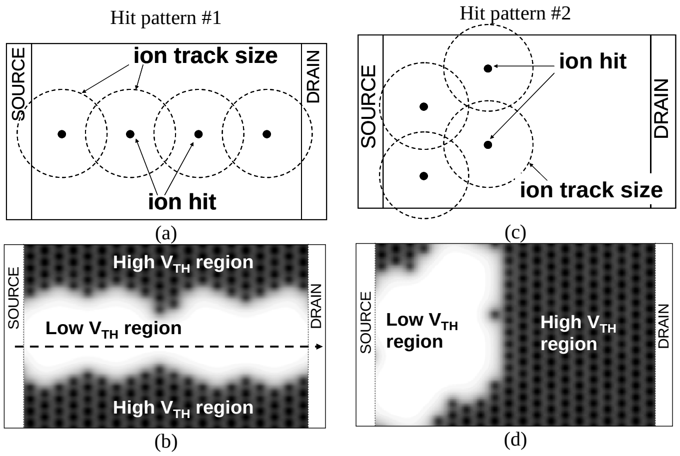


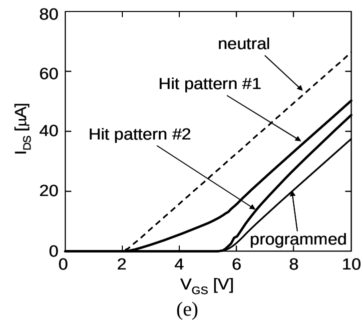


Fig. 7. Comparison between two possible quadruple hit patterns: a) 4 hits perfectly aligned; b) simulated channel resistance of the hit pattern in Fig. a; c) 4 hits close to the source; d) simulated channel resistance of the hit pattern in Fig. c; e) Simulated $I_{DS}$-$V_{GS}$ curves of the neutral, programmed and hit cells of Fig. a-b and c-d.

To simulate the statistical effect of M ion hits on a NCM cell, we used a Monte Carlo approach (detail in the final paper). The main simulation variables were the ion track size and the ion fluence. In Fig. 8 we show a summary of the simulation results. Fig. 8a shows the $V_{TH}$ variation as a function of the ion track size S and for different ion hit numbers. In Fig. 8b we show the simulated average $V_{TH}$ shift after 1-8 hits (S=100nm). Finally, in Fig. 8c we show the comparison between the experimental results and the simulations. We achieved a very good fit of the tail cell distribution by setting the ion track diameter to 87nm.

## VI. CONCLUSIONS

We presented for the first time a model of the heavy ion induced radiation damage on nanocrystal memory cells. Excellent fits of the tail cells distribution are achieved. The model may also take into account the nanocrystal distribution non uniformity and the effect of different programming techniques (CHC, CHISEL, FN), which may produce non uniform charging of the nanocrystals.

The model has been validated with a focused microbeam test. It provides an estimation of both the ion spot size and the average number of ion hits required for achieving a given charge loss. In our irradiation experiments we estimated a ion track size S = 87nm for 50-MeV Cu ions. This model also confirms the good robustness of nanocrystal memories against heavy ion irradiation and their much stronger tolerance than the conventional floating gate based memories. Simulations are running to take into account the nanocrystal distribution non uniformity and to evaluate the impact of non uniform nanocrystal charge distribution.

**Acknowledgement**

The Sandia portion of this work was supported by the Defense Threat Reduction Agency under DTRA IACRO #05-4101I and the U. S. Department of Energy. Sandia is a multiprogram laboratory operated by Sandia Corporation, a Lockheed Martin Company, for the United States Department of Energy's National Nuclear Security Administration under Contract DE-AC04-94AL85000.

**REFERENCES**

[1] S. Lai, IEEE – Non Volatile Memory Techology Conference, p. 6, 1998.
[2] P. J. McNulty, et al., IEEE – Trans. Nucl. Sci. Vol. 49, p. 3016-3021, Dec 2002.
[3] S. M. Guertin, et al., IEEE – Trans. Nucl. Sci. Vol. 53, p. 3518-3524, Dec. 2006
[4] G. Cellere, et al., IEEE – Trans. Nucl. Sci, Vol. 48, p. 2222-2228, Dec. 2001.
[5] R. Bez, Microelectronic Engineering, Vol. 80, p. 249-255, June 2005.
[6] B. De Salvo, et al., IEEE – International Electron Devices Meeting, pp. 26.1.1-26.1.4, 8-10 Dec. 2003.
[7] C. Gerardi, et al., 2004 IEEE International Conference on Integrated Circuit Design and Technology, pp. 37-43, 2004.
[8] A. Cester, et al., IEEE - Transactions on Nuclear Science, Vol. 54, p. 2196 - 2203, 2007

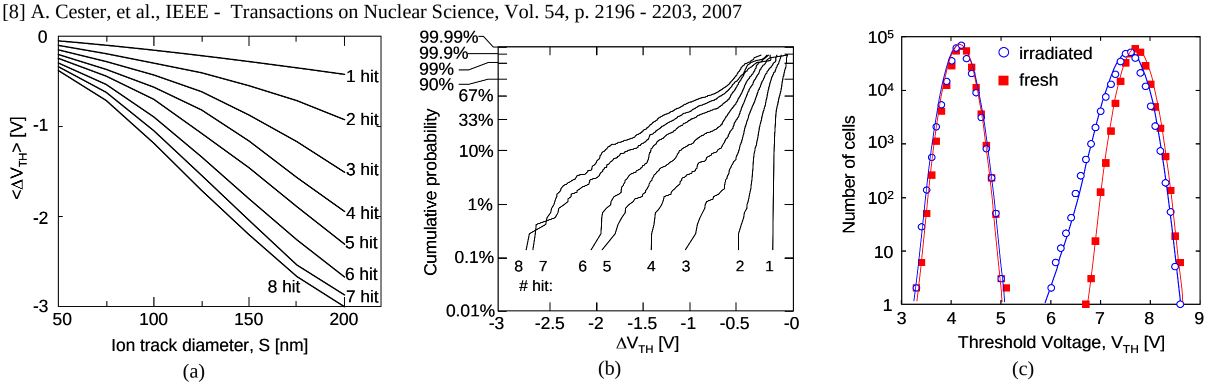


Fig.8. a) Simulated average threshold voltage variation of an irradiated cell as a function of the ion track size and the number of hits. b) Simulated cumulative probability of the threshold voltage variation in an irradiated cell. c) Comparison between the simulations and experimental results of Fig.2. The symbols represent the experimental data and the solid lines represent the theoretical fit.